The Canadian Mineralogist
Vol. 50, pp. 933-942 (2012)
DOI: 10.3749/canmin.50.4.933

AN ASSOCIATION OF SECONDARY Al–Li–Be–Ca–Sr PHOSPHATES IN THE SAN ELÍAS PEGMATITE, SAN LUIS, ARGENTINA

MIGUEL Á. GALLISKI[§]

IANIGLA, CCT–MENDOZA CONICET, Avda. Ruiz Leal s/n, Parque Gral. San Martín, C.C. 330, (5.500) Mendoza, Argentina

PETR ČERNÝ

Department of Geological Sciences, University of Manitoba, Winnipeg, Manitoba R3T 2N2, Canada

MARÍA FLORENCIA MÁRQUEZ-ZAVALÍA

IANIGLA, CCT–MENDOZA CONICET, Avda. Ruiz Leal s/n, Parque Gral. San Martín, C.C. 330, (5.500) Mendoza, Argentina

RON CHAPMAN

Department of Geological Sciences, University of Manitoba, Winnipeg, Manitoba R3T 2N2, Canada

ABSTRACT

The complex association of secondary phosphates from the Li-bearing, rare-element San Elías pegmatite in the Eastern Pampean ranges of Argentina shows widespread albite-hosted dendritic montebrasite in its northern part and lepidolite in the south. This dendritic montebrasite survived low-temperature processes virtually intact, but subrectangular blocks of montebrasite along the margins of quartz core were extensively modified in three stages: (i) two generations of secondary montebrasite intimately intergrown with hydroxylherderite, augelite, and fluorapatite, (acid hydrous fluids, locally channeled, at ~450°–420°C, ~2 kbar); (ii) goyazite–crandallite and hydroxylapatite formed after P–T equilibration between the pegmatite and its host rock along the path of metamorphic cooling, which introduced Ca, Sr and minor S from the host rocks into the pegmatite (at about <300°C); (iii) at a still lower T, the remainder of the primary montebrasite and all of its alteration products were subject to extensive leaching, removal and dispersal of phosphorus, and introduction of Si, generating pseudomorphs consisting mainly of kaolinite, quartz and minor lithian muscovite, K-feldspar (adularia) , and traces of residual microlite as remnants of previous alteration stages.

Keywords: granitic pegmatite, phosphate alteration, montebrasite, hydroxylherderite, augelite, goyazite–crandallite, kaolinization, San Elías, Argentina.

INTRODUCTION

The association of phosphates occurring in granitic pegmatites is quite variable. Primary complex minerals of the transition-metal elements (±Ca, Mg, alkalis) commonly are partially or completely transformed into a population of secondary phases during late-stage, subsolidus hydrothermal reworking, as documented by several authors (*e.g.,* Moore 1973, Hawthorne 1998). Some of the reactions that transform the primary associations are developed during interchange of mobile cations with the host rocks. The associations of secondary minerals show variable parameters of crystallization which, in contrast to the more stable silicate minerals, sensitively document the changes in physicochemical conditions. We describe in this paper a secondary phosphate association where a primary Al–Li phase was reworked by hydrothermal fluids, producing a sequence of assemblages with Al–Li, Al–Be, Al–Sr, Ca–Al, and Ca phosphates.

THE PARENT PEGMATITE

The phosphate assemblage is hosted by the San Elías pegmatite, located in the Sierra de la Estanzuela, departamento Chacabuco, San Luis province, República

§ *E-mail address*: galliski@mendoza-conicet.gov.ar

Argentina, approximately at 31°51'S latitude and 65°06' W longitude (Fig. 1). The pegmatite is emplaced in a quartz–mica schist of medium metamorphic grade belonging to the Conlara Metamorphic Complex (Sims *et al*. 1997), probably of Lower Paleozoic age, which is locally tourmalinized in contact with the hanging wall of the pegmatite body.

San Elías is an LCT-family, rare-element class pegmatite according to the classification of Černý & Ercit (2005). The internal structure and mineralogy of the dike were initially described in general by Angelelli & Rinaldi (1963) and Herrera (1963). More recently, Galliski *et al*. (1999) characterized its principal features and provisionally classified it as a lepidolite-subtype pegmatite, but montebrasite also turned out to be an important component (Galliski *et al*. 2011). The pegmatite is a tabular body, 140 m long, striking N–S and steeply dipping to the east. It is only partially exposed because the eastern side is covered by Quaternary loess, and consequently the width of the partial outcrop varies between 15 and 27 m.

The pegmatite is zoned, with border, wall, intermediate and core zones (Fig. 1). The *border* and *wall zones* are fine- and medium-grained rocks, respectively, principally composed of plagioclase ($An_{\sim 15}$), quartz and muscovite, and only exposed in the western part of the pegmatite. The *intermediate zone* has a medium to coarse grain-size, with K-feldspar, quartz, and platy albite as main minerals; pale yellow beryl and Nb–Ta minerals are rare. In the southern part of the pegmatite, there is a poorly defined intermediate subzone composed of platy albite and small crystals and subhe-

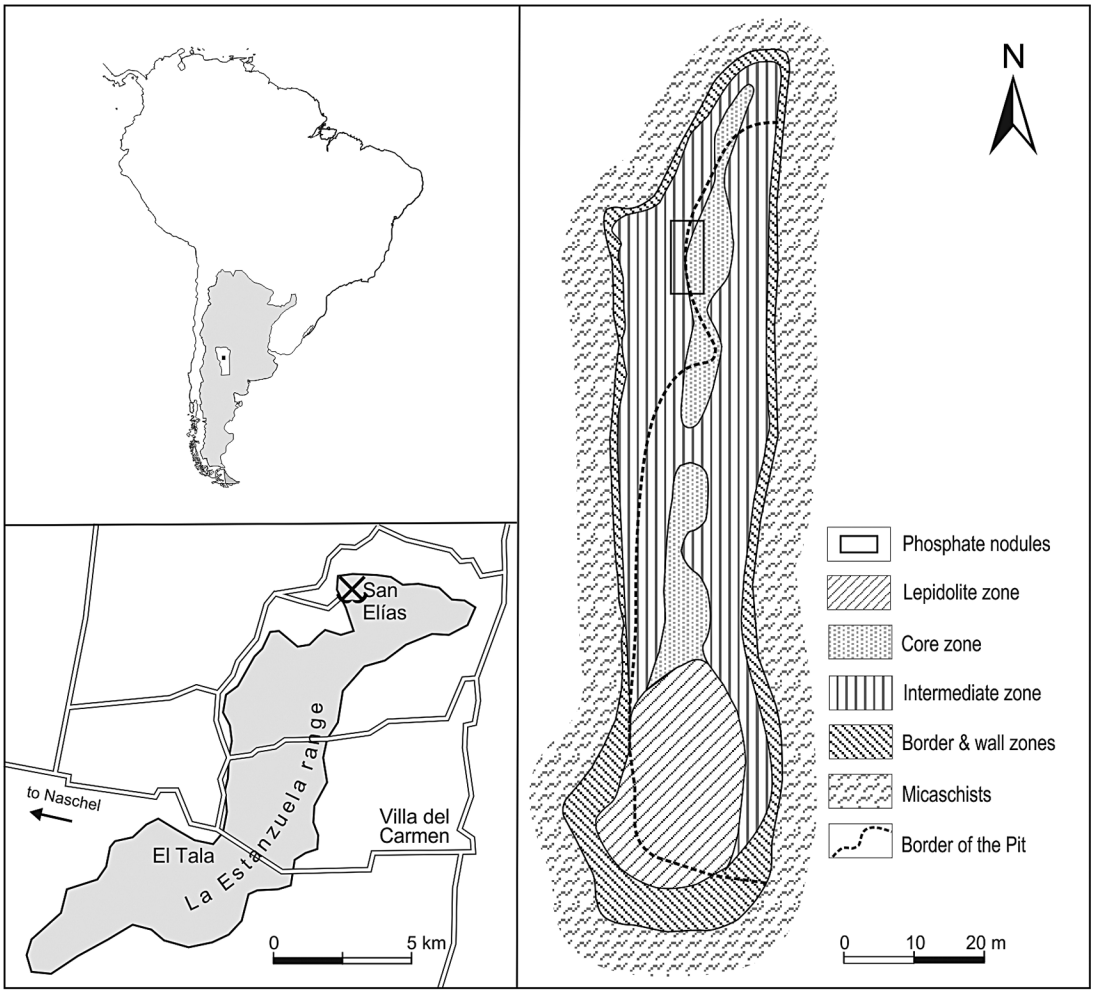

FIG. 1. Schematic map of the San Elías pegmatite with the location of the pegmatite and the phosphate nodule.

dral grains of montebrasite in dendritic aggregates, with blue, green, colorless and pink tourmaline as the principal accessory mineral (Toubes *et al.* 1973). In contrast, gray, pink or purple, fine-grained to massive lepidolite is widespread in this subzone. The *core* is irregular and is composed of quartz with a few large euhedral crystals of K-feldspar. In the platy-albite-bearing *core–margin* assemblage, there are abundant vugs with late-stage growth of quartz, cookeite, apatite and a mineral of the herderite group (Gay & Hillar 1972). Mostly in the northern half of the pegmatite, the core margin also hosts scattered subrectangular blocks (up to ~25 cm in size) of an unknown phase completely replaced by a soft, white, kaolinized material and a hard phosphate nodule that are the main focus of the present study.

Except for the montebrasite, apatite and hydroxylherderite, other phosphates are very scarce in San Elías, and only a single sample of Mn–Fe–Li phosphates was found on the dumps.

The pegmatite was opened in 1957 to explore its potential for beryl and lepidolite, but after extensive initial work, the activity ceased. Several quarries were developed at this time along strike, and these provided good exposure of the intermediate zone. However, in recent years, it was realized that the Al–Li phosphates widely disseminated in the feldspars considerably reduced the melting point of the pulverized rock. The pegmatite was intensively mined for this high-quality ceramic material and a quartz by-product, and the excellent exposure of the phosphate assemblage was largely destroyed.

Petrography of the Phosphates and Alteration Products

In the west wall of the main quarry of the northern part of the San Elías pegmatite (Fig. 1), the exposed units are mostly the intermediate zone and the quartz core zone. The intermediate zone consists here of K-feldspar in coarse crystals, quartz, platy albite and muscovite. In some parts of this zone, an irregular subzone composed mainly of platy albite and montebrasite with minor tourmaline is present. Dendritic montebrasite is commonly intergrown here with cream-colored platy albite (Fig. 2a); the matrix of platy albite contains abundant, skeletal, white crystals of montebrasite and some small darker crystals of blue to green tourmaline (Fig. 2b).

South of the dendritic montebrasite, the subrectangular white blocks and the white nodule are located at the core–margin transition. The ovoid nodule is surrounded by a halo of soft altered rock (Figs. 2c, d). This halo is closely similar to the argillaceous material that forms the white subrectangular blocks (Fig. 3a). X-ray powder diffraction and EPM analyses of these argillaceous blocks reveal dominant kaolinite and quartz, with minor muscovite, illite, K-feldspar, fluorapatite, hydroxylapatite, lithian muscovite, lepidolite and microlite. In some blocks that appear deformed, irregular veinlets of quartz cross-cut the white aggregate, porcelaneous or soft depending on the degree of pervasive silicification. Some thin veinlets stained by "limonite" suggest the presence of a roughly rectangular network of cleavage or parting in the apparent primary phase (Fig. 3b).

The ovoid nodule, 15 by 10 cm in size, is white with a light gray to light blue tinge in some parts and very tenacious (Fig. 2d). It consists of a crystalline aggregate with decreasing grain-size from 1 mm to 0.6 mm from the outer part toward the center. The association comprises crystals of montebrasite intergrown with augelite, fluorapatite, hydroxylherderite, goyazite–crandallite, hydroxylapatite and quartz (Table 1, Figs. 4, 5).

Mineralogy of the Ovoid Nodule

Experimental methods

Electron-microprobe analyses of the phosphate minerals and paragenetically related phases were carried out in the wavelength-dispersion mode on a Cameca Camebax SX50 equipment, with a beam diameter of 3 μm and an acceleration potential of 15 kV. A sample current of 20 nA measured on Faraday cup and a counting time of 20 s were used for Na, Mg, Al, Si, P, S, Cl, K, Ca, V, Mn, Fe, As, Sr, Y, Ba, La, Ce, Nd, Pb, Bi, Th and U. For F, a counting time of 30 s was used. The standards used are apatite (Ca*K*α, P*K*α, F*K*α), albite (Na*K*α), olivine (Mg*K*α), andalusite (Al*K*α), diopside (Si*K*α), PbS (S*K*α), tugtupite (Cl*K*α), orthoclase (K*K*α), VP_2O_7 (V*K*α), spessartite (Mn*K*α), fayalite (Fe*K*α), pyromorphite (As*L*α), $SrTiO_3$ (Sr*L*α), YTAP (Y*L*α), barite (Ba*L*α), $LaVO_4$ (La*L*α), $CePO_4$ (Ce*L*α), $NdPO_4$ (Nd*L*α), PbTe (Pb*M*α), Bi_2Se_3 (Bi*M*β), ThO_2 (Th*M*α) and UO_2 (U*M*β). Data were reduced using the PAP routine of Pouchou & Pichoir (1985). X-ray powder-diffraction data of the different assemblages were collected using Philips PW 1710 equipment.

Montebrasite, $LiAlPO_4(OH)$

Montebrasite is present in two generations: (i) scarce large (3–4 mm) crystals generally somewhat irregular and corroded, that show localized alteration, and (ii) thin, tabular, euhedral, small (<2 mm), clear crystals, widely distributed with a random orientation except for some radial clusters (Fig. 4a). Both generations show polysynthetic twinning. The first generation of montebrasite is partially replaced by the second, locally by augelite, and more commonly by goyazite–crandallite. The chemical composition (Table 1) of both generations of montebrasite is virtually identical, with very low F content indicative of almost end-member montebrasite

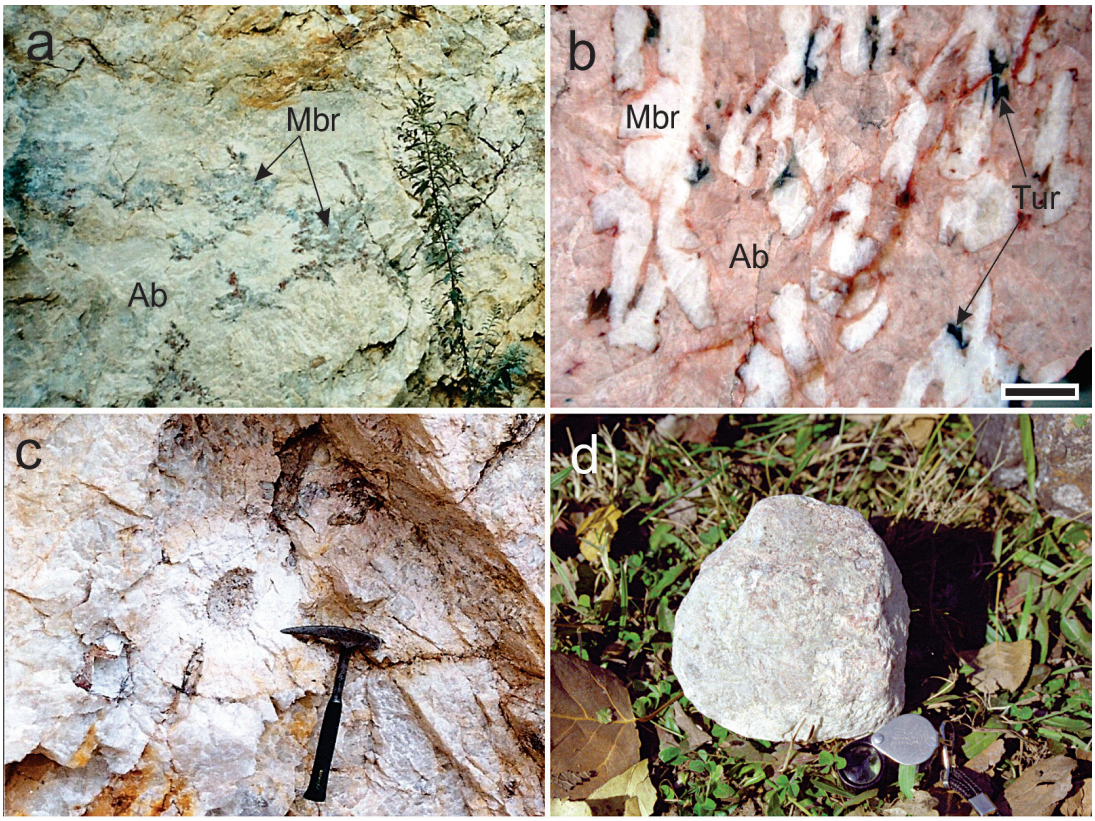

FIG. 2. a. Dendritic primary montebrasite included in albite; the branch of bush to the right is approximately 1 m long. b. Polished section showing skeletal montebrasite in an albite groundmass with accessory tourmaline and traces of columbite; scale bar is 1 cm. c. Cavity left after extraction of the nodule of the phosphates studied; hammer length is 33 cm. d. Nodule of the phosphate association; the hand lens is 2.5 cm diameter.

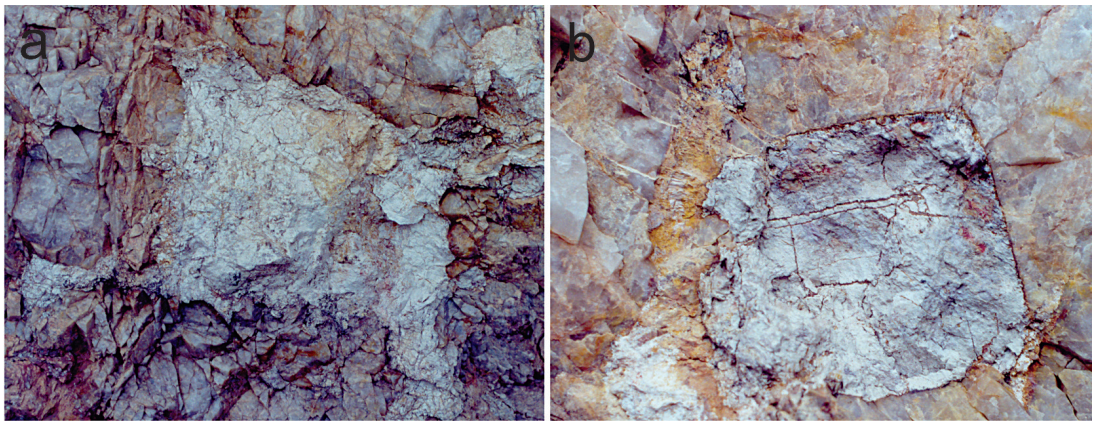

FIG. 3. a. Subrectangular block consisting mainly of quartz and kaolinite at the margin of the intermediate zone and the quartz core. The bottom edge of the block is 70 cm long. b. Subrectangular block of a quartz + kaolinite aggregate, criss-crossed by stained quartz iron-oxide veinlets in the margin of the quartz core. The block is about 20 cm along the vertical edge on the right-hand side. Note the radial cracks in the quartz matrix along the upper and left-hand contact.

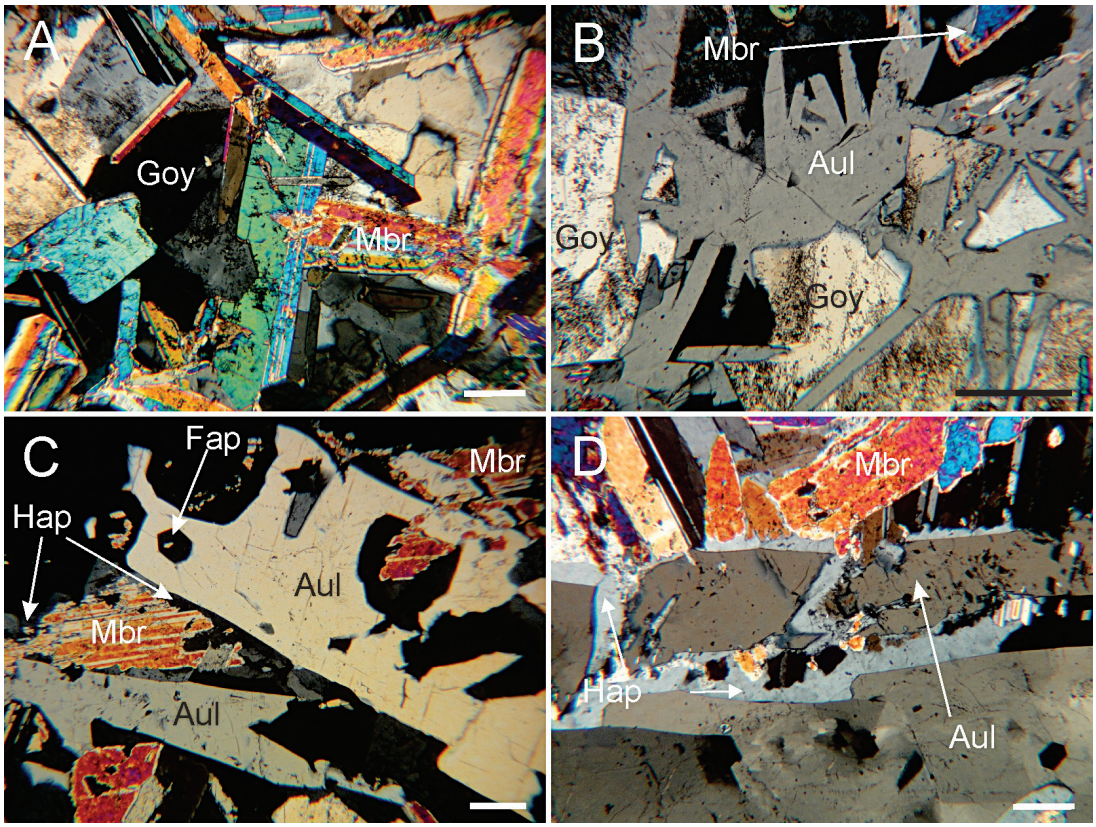

FIG. 4. Photomicrograph of the phosphate association in the nodule; scale bar is 200 μm. a. Twinned montebrasite crystals of the second generation, locally partially radial with interstitial goyazite–crandallite. b. Network formed by laths of augelite in optical continuity, and smaller tabular crystals of montebrasite, embedded in a crystal of goyazite–crandallite. c. Corroded crystal of montebrasite from the first generation, cross-cut by a tabular crystal of augelite that includes a euhedral crystal of fluorapatite. Interstitial hydroxylapatite fringe separates montebrasite from augelite. d. Montebrasite of the second generation cross-cut by a tabular crystal of augelite, broken and cemented by interstitial hydroxylapatite.

($Amb_{\sim 1.5}$), uniform contents of major components and ~0.01 wt.% Na_2O.

Augelite, $Al_2PO_4(OH)_3$

Augelite forms euhedral laths of up to 3 mm in length, very clear under the polarizing microscope (Figs. 4b, c, d). Locally, the lamellar crystals are grouped in subparallel aggregates attached to a major lath. Augelite cuts across and clearly replaces the major crystals of the first generation of montebrasite; the second generation of montebrasite is usually not replaced or only slightly affected. In turn, goyazite–crandallite commonly corrodes the augelite crystals. However, contact between these minerals is uncommon, as they are generally separated by fringes of hydroxylapatite. The chemical composition of augelite (Table 1) is quite constant in terms of major oxides.

Hydroxylherderite, $CaBePO_4(OH)$

Hydroxylherderite occurs as a minor phase in subhedral, tabular crystals up to 1 mm in size, associated with the second generation of montebrasite and usually enveloped by augelite. Hydroxylherderite persists in the argillized subrectangular blocks associated with augelite, goyazite, and remnant microlite embedded in kaolinite cross-cut by quartz veinlets. Its chemical composition (Table 1) shows P slightly below the ideal content and Ca close to it or slightly in excess. Silicon, Al, Mn and Fe are present as minor elements; Sr is very low. The F content of this mineral is in the order of 1.52 to 1.87 wt.%, corresponding to a hydroxylherderite composition. Previously, Gay & Hillar (1972) described herderite as a late-stage mineral in crystals up to 2 mm covering cavities in albite from this pegmatite. The chemical analysis given by these authors did not include

fluorine and showed 7.40 wt.% H_2O corresponding to hydroxylherderite, which is the most frequently encountered member of the series.

Goyazite–crandallite, $SrAl_3(PO_4)(PO_3OH)(OH)_6$ – $CaAl_3(PO_4)(PO_3OH)(OH)_6$

Members of this series occur occasionally in euhedral to subhedral crystals or radial aggregates, filling interstices between other minerals (Figs. 4a, b, 5b, c, d). They commonly replace augelite, and less commonly, montebrasite. The crystals are more common in the external part of the nodule; inside it, goyazite–crandallite forms irregular veinlets or patches that usually replace montebrasite (Figs. 5c, d). The chemical composition (Table 1) shows sulfur up to 0.195 *apfu* (3.30 wt.% SO_3) predominantly in goyazite members. Strontium ranges from 15.60 wt.% of SrO (0.711 *apfu*) in goyazite to 0.98% wt.% (0.040 *apfu*) in crandallite. Iron and Na contents are slightly higher, and F shows some predominance in the goyazite-rich phases.

Fluorapatite and hydroxylapatite, $Ca_5(PO_4)_3F$ – $Ca_5(PO_4)_3OH$

Both members of the apatite supergroup are present in the nodule. Fluorapatite occurs as small euhedral crystals usually enclosed in augelite, possibly contemporaneous with it (Fig. 4c). The chemical composition is quite uniform, with fluorine contents corresponding to the end member and with a content of MnO that attains almost 3 wt.% (Table 1). Hydroxylapatite is more widespread, distributed usually in thin veins, or fringes on other minerals and anhedral grains (Figs. 4c, d, 5a, b, c). Hydroxylapatite commonly replaces augelite or forms the last interstitial phosphate phase among other minerals of the nodule. Its chemical composition is variable, and shows higher Cl and S contents than

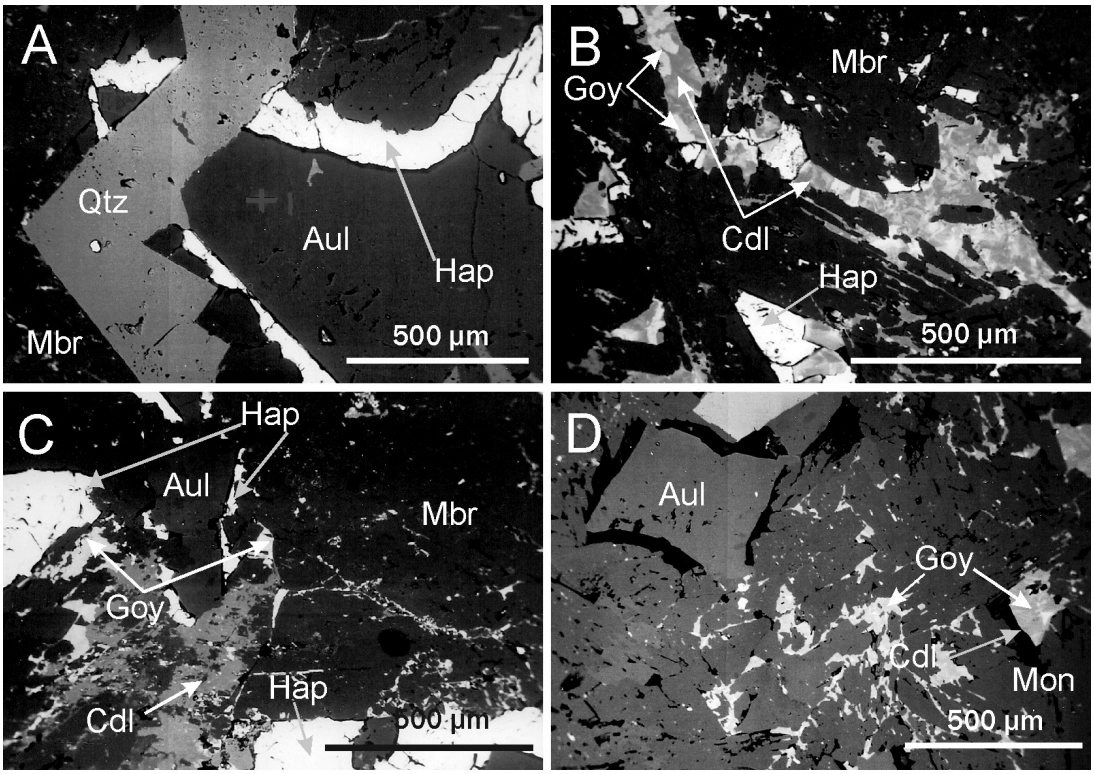

FIG. 5. Back-scattered electron images of the phosphate association in the nodule. a. Montebrasite cross-cut by augelite with an intervening rim of hydroxylapatite; a late-stage irregular veinlet of quartz cuts across the first two minerals. b. Crystal of montebrasite of the first generation is partially replaced by an irregular veinlet of secondary goyazite, in turn disrupted and followed by the more widespread crandallite. c. Montebrasite of the first generation locally replaced by hydroxylapatite in contact with augelite, and a late-stage patchy replacement of crandallite with minor goyazite. d. Broken lath of augelite and montebrasite with irregular replacement by goyazite–crandallite.

TABLE 1. CHEMICAL COMPOSITION OF THE PHOSPHATES IN THE SAN ELÍAS PEGMATITE

	Mbr I	Mbr II	Aul	Hhd	Cdl	Goy	Fap	Hap
	a		b	c	d		e	
n	5	5	8	5	8	7	6	6
SO_3 wt.%	0.01 (0.01)	0.01 (0.01)	0.02 (0.02)	0.02 (0.02)	1.07 (1.25)	1.87 (1.07)	0.07 (0.08)	0.15 (0.10)
P_2O_5	49.55 (0.49)	50.37 (0.37)	35.72 (0.31)	39.71 (1.79)	31.73 (1.50)	27.13 (2.82)	40.87 (0.86)	41.58 (0.35)
SiO_2	0.37 (0.43)	0.02 (0.03)	---	0.51 (0.33)	0.42 (0.86)	1.92 (2.69)	0.27 (0.42)	0.00 (0.00)
CeO_2	---	---	---	---	0.08 (0.09)	0.02 (0.03)	---	---
Al_2O_3	34.44 (0.13)	34.93 (0.27)	49.46 (0.16)	0.26 (0.13)	33.44 (1.34)	31.94 (0.65)	0.08 (0.18)	0.01 (0.01)
FeO	0.02 (0.01)	0.02 (0.02)	0.03 (0.02)	0.14 (0.08)	0.10 (0.12)	0.10 (0.10)	0.21 (0.11)	0.14 (0.04)
MnO	---	---	0.01 (0.01)	0.73 (0.46)	0.12 (0.24)	0.02 (0.02)	1.00 (1.07)	1.66 (0.33)
MgO	---	---	---	---	0.16 (0.34)	0.01(0.02)	---	---
CaO	0.02 (0.02)	0.01 (0.01)	0.01 (0.01)	32.76 (0.39)	9.31 (2.19)	4.70 (1.03)	51.46 (1.14)	52.96 (0.43)
SrO	0.02 (0.04)	0.01 (0.02)	0.01 (0.02)	0.05 (0.04)	5.50 (4.02)	13.20 (1.66)	0.02 (0.02)	0.04 (0.05)
BaO	---	---	0.01 (0.02)	---	0.33 (0.29)	0.08 (0.07)	0.01 (0.01)	0.04 (0.04)
Na_2O	---	---	---	0.06 (0.11)	0.22 (0.24)	0.02 (0.05)	0.05 (0.08)	0.03 (0.03)
K_2O	0.09 (0.11)	0.00 (0.00)	0.00 (0.01)	0.06 (0.04)	0.09 (0.10)	0.02 (0.01)	0.05 (0.05)	0.01 (0.01)
F	0.15 (0.17)	0.16 (0.06)	0.01 (0.01)	1.32 (1.73)	0.14 (0.16)	0.29 (0.36)	3.73 (0.36)	0.42 (0.14)
Cl	0.01 (0.01)	0.00 (0.00)	---	0.03 (0.03)	0.00 (0.00)	0.01 (0.01)	0.01 (0.01)	1.14 (0.51)
Li_2O *	10.33 (0.05)	10.47 (0.07)	---	---	---	---	---	---
BeO *	---	---	---	14.46 (0.42)	---	---	---	---
H2O *	6.17 (0.06)	6.24 (0.05)	13.34 (0.07)	4.58 (0.40)	14.28 (0.45)	13.35 (0.19)	0.06 (0.13)	1.27 (0.18)
O=F	-0.06 (0.07)	-0.07 (0.02)	0.00 (0.01)	-0.56 (0.31)	-0.06 (0.07)	-0.12 (0.15)	-1.57 (0.15)	-0.18 (0.06)
O=Cl	0.00 (0.00)	0.00 (0.00)	---	-0.01 (0.01)	0.00 (0.00)	0.00 (0.00)	0.00 (0.00)	-0.26 (0.12)
Total	101.12 (0.29)	102.19 (0.67)	98.62 (0.51)	94.12 (2.25)	96.89 (1.46)	94.54 (1.99)	98.77 (1.33)	99.28 (0.50)
S *apfu*	0.000	0.000	0.001	0.001	0.058	0.109	0.005	0.009
P	1.007	1.012	1.019	0.968	1.964	1.789	2.953	2.994
Si	0.009	0.000	---	0.015	0.032	0.147	0.023	0.000
Sum	---	---	---	---	2.053	2.045	---	---
Ce	---	---	---	---	0.002	0.000	---	---
Al	0.974	0.977	1.964	0.009	2.881	2.931	0.016	0.002
Fe^{2+}	0.000	0.000	0.001	0.003	0.006	0.007	0.007	0.008
Mn^{2+}	---	---	0.000	0.018	0.007	0.001	0.101	0.119
Mg	---	---	---	---	0.017	0.001	---	---
Sum	---	---	---	---	2.915	2.943	---	---
Ca	0.001	0.000	0.000	1.011	0.727	0.392	4.899	4.854
Sr	0.000	0.000	0.000	0.001	0.237	0.596	0.001	0.002
Ba	---	---	0.000	---	0.009	0.003	0.000	0.001
Na	---	---	---	0.003	0.030	0.003	0.008	0.005
K	0.003	0.000	0.000	0.002	0.008	0.002	0.006	0.001
Sum	---	---	---	---	1.011	0.995	---	---
F	0.011	0.012	0.001	0.120	0.033	0.070	1.007	0.114
Cl	0.000	0.000	---	0.001	0.000	0.001	0.001	0.165
Be	---	---	---	1.000	---	---	---	---
Li	0.997	1.000	---	---	---	---	---	---
H	0.988	0.988	2.999	0.878	6.967	6.929	0.031	0.721
O	4.988	4.988	6.999	4.878	13.967	13.929	11.992	12.721
CATSUM	2.993	2.992	2.987	3.031	5.981	5.984	8.018	7.993

The analyses were made with an electron microprobe. * Determined by stoichiometry. [a] Formula contents based on five anions, assuming 1(Li + Na + K) and 1(OH + F + Cl) per formula unit. [b] Formula contents based on seven anions per formula unit. [c] Formula contents based on five anions, assuming 1 Be and 1 (OH, F, Cl) per formula unit. [d] Formula contents based on 14 atoms of oxygen; the H_2O content was calculated determined by stoichiometry, assuming 5 (OH+F+Cl) and 1 H_2O per formula unit. [e] Formula contents based on 13 anions; the H_2O was calculated assuming 1(OH, F, Cl) per formula unit. Symbols used: Mbr I: montebrasite I, Mbr II: montebrasite II, Aul: augelite, Hhd: hydroxylherderite, Cdl: crandallite, Goy: goyazite, Fap: fluorapatite, Hap: hydroxylapatite, *n*: number of analyses.

fluorapatite, similar contents of Mn, and low contents of Sr. Silica is also comparatively higher, up to 4 wt.%.

Quartz

This is the very last phase to have precipitated in the nodule, forming irregular small fillings between diverse phosphates.

Discussion

The original primary phase(s) that built the nodule and the blocks were probably of magmatic origin, *i.e.*, OH-dominant members of the amblygonite–montebrasite series that were replaced during the hydrothermal stage by secondary phosphates. This assumption come from several paragenetic and textural features considered collectively: the occurrence of square blocks or nodules included in the inner intermediate or border of the core zone (*e.g.*, Quensel 1956, Černá *et al.* 1972; Fig. 1), the palimpsestic evidence of *quasi*-orthogonal cleavage of the subrectangular blocks, the presence of the first generation of montebrasite in the nodule that could represent remnants of a primary phase, and the convergence of the ultimate products of alteration of both the blocks and the nodule.

The textural relationships of all the minerals show that both generations of montebrasite, hydroxylherderite, fluorapatite and augelite were followed by goyazite–crandallite, and finally hydroxylapatite and quartz. Similar occurrences of Al-rich phosphates have been described in other pegmatites, generally as secondary derivatives of amblygonite–montebrasite phases, among which are Palermo #1 (Mrose 1953), the White Picacho district, especially the Midnight Owl pegmatite (London & Burt 1982), Buranga (Daltry & von Knorring 1998, Fransolet 1989), and Okatjimukuju (Baldwin *et al.* 2000). These assemblages are somewhat variable at different localities due to Na, Ca or Ba metasomatism (Moore 1973), and also contain palermoite, brazilianite, lacroixite, gorceixite, bertossaite or gatumbaite. London & Burt (1982) established a general sequence of alteration for montebrasite: primary montebrasite → secondary montebrasite → hydroxylapatite + *crandallite* → hydroxylapatite + muscovite + brazilianite + *augelite* + scorzalite + kulanite + wyllieite → muscovite → carbonate–apatite (with tentative identification of italicized species). Baldwin *et al.* (2000) established an alteration sequence for Karibib pegmatites with amblygonite → montebrasite and low-F montebrasite – "natromontebrasite" (now discredited; Fransolet *et al.* 2007) – fluorapatite → brazilianite → crandallite + goyazite + gorceixite – hydroxylapatite + muscovite. Some minerals of this assemblage, such as goyazite–crandallite, are not specific to granitic pegmatites because they also occur in some albitized granites such as Beauvoir (Charoy *et al.* 2003).

The conversion of the primary montebrasite to the fine-grained hydrothermal end-member montebrasite began after completion of magmatic crystallization, when the postmagmatic fluids became extremely depleted in F. The temperature was possibly about 450°C, with the upper limit defined by the end of magmatic crystallization, and the lower, by the stability of augelite. Wise & Loh (1976) showed experimentally in the system Al_2O_3–$AlPO_4$–H_2O for P–T between 400–600°C and 0.5–3 kbar that augelite + berlinite are stable between <520° and 420°C at approximately 2 kbar, which is a rough estimate of the emplacement pressure of the San Elías pegmatite. At lower T, augelite + berlinite become unstable and are replaced by trolleite; at T higher than ~500°C, the stable association is berlinite + corundum + vapor. In addition, Drüppel *et al.* (2007) showed experimentally that in the same system below 200°C, the stable phases are variscite and metavariscite, minerals that are absent in the association studied. These data bracket the conditions of formation of augelite, restricted to the approximate range of 420°–450°C, and strongly suggest an origin by crystallization from an acid P-rich hydrothermal fluid at the late stage of evolution of the pegmatite, after the formation of the secondary montebrasite and close to the crystallization of hydroxylherderite.

The hydroxylherderite in the assemblage of secondary phosphates raises the question of the provenance of its Be content. Beryl in the San Elías pegmatite does not show any signs of corrosion or replacement, thus some of the Be must have been kept preserved, and its activity raised in the postmagmatic fluids; London & Evensen (2002) discussed the diversity of factors influencing the fate of Be throughout pegmatite consolidation. The presence of minor but widespread hydroxylherderite in vugs strung along the core margin is symptomatic in this respect.

The formation of goyazite–crandallite and hydroxylapatite occurs at a different stage marked by the appearance of Sr, Ca, S, and other cations that interact with the P–Al-bearing fluids produced by destabilization of primary montebrasite and the feldspars. Charoy *et al.* (2003) showed that the local excess of Sr in the Beauvoir granite is provided by fluids circulating in an open system. This fluid would leach these elements from the host rock (in the San Elías case, quartz–mica schists) after the re-equilibration of pegmatite and host rock along the P–T paths of metamorphic cooling that followed the magmatic crystallization.

The final product of the primary montebrasite blocks, once the P content of the assemblage was leached, is the fine-grained argillaceous material dominantly formed by kaolinite and quartz, with subordinate to minor quantities of muscovite, illite, K-feldspar, hydroxylapatite, fluorapatite, lithian muscovite, lepidolite and microlite, which are remnants from previous episodes. The fluids must have been necessarily channeled along

fractures and did not move pervasively because, just a few meters away from the altered nodules, fresh skeletal montebrasite is found.

Conclusions

Intergrowths of fine-grained montebrasite, hydroxylherderite, augelite, hydroxylapatite, goyazite–crandallite and quartz from the San Elías pegmatite form a secondary association produced by the non-equilibrium subsolidus alteration of the primary Al–Li phosphate, blocky montebrasite. The multiple-stage process triggered by late-stage acidic fluids below ~450°C generated initially (i) secondary montebrasite and hydroxylherderite, followed at lower T, after the consumption and dispersal of Li, by fluorapatite and, at increasing H_2O activity between 450° and 420°C, by augelite. The formation of (ii) interstitial goyazite–crandallite and hydroxylapatite at a T lower than ~300°C marks the equilibration of pressure between the solidifying pegmatite and the host rock, and the influx of fluids with cations derived from sources external to the pegmatite. (iii) After this re-equilibration, facilitated by hydrogen metasomatism, the decay of the original blocky montebrasite further evolved by extreme leaching and cation exchange to a mass of very fine-grained kaolinite, quartz, with remnants of lithian muscovite ($2M_1$), K-feldspar (of adularia habit), and fluorapatite from previous stages of alteration and some isolated residual grains of microlite. Figure 6 shows the sequence of mineral formation schematically.

Acknowledgements

This study was made possible by the support of CONICET and FONCYT from Argentina through grants PIP 5907 and 22–21637 respectively to M.A. Galliski. The Natural Sciences and Engineering Research Council of Canada provided Major Installation and Research Grants to P. Černý and Major Equipment, Research and Infrastructure grants to F.C. Hawthorne, which supported the laboratory work at the

Stage	Process	Mineral association		Conditions
		Ovoid nodule	Square blocks	
Magmatic		Montebrasite I	*Montebrasite I?* Microlite	
Magmatic-Hydrothermal transition	PO_4^{3-}, Li, Be reworking	Montebrasite II Hydroxylherderite	Hydroxylherderite	450ºC?
Hydrothermal	Acid PO_4^{3-} rich fluids	Augelite Fluorapatite	*Augelite?* Fluorapatite	~450º-420ºC
	SiO_4H_4 rich fluids		K-feldspar (adularia) Lithian muscovite($2M_1$)	~400º-300ºC
	Sr, Ca, S input from leaching of the host rock	Crandallite Goyazite Hydroxylapatite		~300º-200ºC ~1.8 kbar
	Intermediate SiO_4H_4, low pH fluids	Quartz	Kaolinite Quartz	~250º-100ºC ~1 kbar?

FIG. 6. Schematic sequence of mineral formation in the ovoid nodule and the square blocks. The names of minerals shown in italics are probable precursors that were totally replaced.

University of Manitoba. The authors are grateful for the thorough reviews of the manuscript by Pietro Vignola and Frédéric Hatert, and for the editorial suggestions and corrections made by Guest Editor Milan Novák and the Editor, Robert F. Martin.

References

Angelelli, V. & Rinaldi, C.A. (1963): Yacimientos de minerales de litio de las provincias de San Luis y Córdoba. *Comisión Nacional de Energia Atómica* **91** (unpubl. rep.).

Baldwin, J.R., Hill, P.G., von Knorring, O. & Oliver, G.J.H. (2000): Exotic aluminum phosphates, natromontebrasite, brazilianite, goyazite, gorceixite and crandallite from rare-element pegmatites in Namibia. *Mineral. Mag.* **64**, 1147-1164.

Černá, I., Černý, P. & Ferguson, R.B. (1972): The Tanco pegmatite at Bernic Lake, Manitoba. III. Amblygonite–montebrasite. *Can. Mineral.* **11**, 643-659.

Černý, P. & Ercit, T.S. (2005): The classification of granitic pegmatites revisited. *Can. Mineral.* **43**, 2005-2026.

Charoy, B., Chaussidon, M., Le Carlier De Veslud, C. & Duthoud, J.L. (2003): Evidence of Sr mobility in and around the albite–lepidolite–topaz granite of Beauvoir (France): an in-situ ion and electron probe study of secondary Sr-rich phosphates. *Contrib. Mineral. Petrol.* **145**, 673-690.

Daltry, V.D.C. & von Knorring, O. (1998): Type-mineralogy of Rwanda with particular reference to the Buranga pegmatite. *Geologica Belgica* **1**, 9-15.

Drüppel, K., Hösch, A. & Franz, G. (2007): The system Al_2O_3–P_2O_5–H_2O at temperatures below 200°C: experimental data on the stability of variscite and metavariscite $AlPO_4$•$2H_2O$. *Am. Mineral.* **92**, 1695-1703.

Fransolet, A.-M. (1989): The problem of Na–Li substitution in primary Li–Al phosphates: new data on lacroixite, a relatively widespread mineral. *Can. Mineral.* **27**, 211-217.

Fransolet, A.-M., Fontan, F. & de Parseval, P. (2007): Natromontebrasite, a discredited mineral species. *Can. Mineral.* **45**, 391-396.

Galliski, M.Á., Černý, P., Márquez-Zavalía, M.F. & Chapman, R. (1999): Ferrotitanowodginite, $Fe^{2+}TiTa_2O_8$, a new mineral of the wodginite group from the San Elías pegmatite, San Luis, Argentina. *Am. Mineral.* **84**, 773-777.

Galliski, M.Á., Černý, P., Márquez-Zavalía, M.F. & Chapman, R. (2011): Association of secondary Al–Li–Be–Ca–Sr phosphates in the San Elías pegmatite, San Luis, Argentina. *Asoc. Geol. Arg. Serie D. Pub. Esp.* **14**, 95-97.

Gay, H.D. & Hillar, N. (1972): Herderita de la mina San Elías, provincia de San Luis. *Rev. Asoc. Geol. Arg.* **37**, 378-382.

Hawthorne, F.C. (1998): Structure and chemistry of phosphate minerals. *Mineral. Mag.* **62**, 141-164.

Herrera, A.O. (1963): Las pegmatitas de la Provincia de San Luis, Estructura, mineralogía y génesis. *Rev. Asoc. Geol. Argentina* **18**, 43-71.

London, D. & Burt, D.M. (1982): Alteration of spodumene, montebrasite and lithiophilite in pegmatites of the White Picacho District, Arizona. *Am. Mineral.* **67**, 97-113.

London, D. & Evensen, J.M. (2002): Beryllium in silicic magmas and the origin of beryl-bearing pegmatites. *In* Beryllium: Mineralogy, Petrology, and Geochemistry (E.S. Grew, ed.). *Rev. Mineral. Geochem.* **50**, 445-486.

Moore, P.B. (1973): Pegmatite phosphates: descriptive mineralogy and crystal chemistry. *Mineral. Rec.* **4**, 103-130.

Mrose, M.E. (1953): Palermoite and goyazite, two strontium minerals from the Palermo mine, North Groton, New Hampshire. *Am. Mineral.* **38**, 354 (abstr.).

Pouchou, J.L. & Pichoir, F. (1985): "PAP" $\phi(\rho Z)$ correction procedure for improved quantitative microanalysis. *In* Microbeam Analysis (J.T. Armstrong, ed.). San Francisco Press, San Francisco, California (104-106).

Quensel, P. (1956): The paragenesis of the Varuträsk pegmatite, including a review of its mineral assemblage. *Arkiv Mineral. Geol.* **2**, 9-125.

Sims, J.P., Skinner, R.G., Stuart-Smith, P.G. & Lyons, P. (1997): Geology and metallogeny of the Sierras de San Luis y Comechingones 1:250.000 mapa sheet. Provinces of San Luis and Córdoba. *Anales XVIII , Instituto de Geología y Recursos minerales,* SEGEMAR, Buenos Aires, Argentina.

Toubes, R.O., Rinaldi, C.A. & Figini, A.J. (1973): Turmalinas de color de la República Argentina. *Actas V Congreso Geológico Argentino* (*Villa Carlos Paz*) **I**, 261-269.

Wise, W.S. & Loh, S.E. (1976): Equilibria and origin of minerals in the system Al_2O_3–$AlPO_4$–H_2O. *Am. Mineral.* **61**, 409-413.

Received July 14, 2011, revised manuscript accepted July 10, 2012.